Effect of formamidinium/cesium substitution and PbI2 on the long-term stability of triple-cation perovskites

Shukla, Shashwat; Shukla, Sudhanshu; Lew, Jia Haur; Dintakurti, Sai S.H.; Han, Guifang; Priyadarshi, Anish; Baikie, Tom; Mhaisalkar, Subodh Gautam; Mathews, Nripan

2017

Shukla, S., Shukla, S., Lew, J. H., Dintakurti, S. S. H., Han, G., Priyadarshi, A., . . . Mathews, N. (2017). Effect of formamidinium/cesium substitution and PbI2 on the long-term stability of triple-cation perovskites. ChemSusChem, 10(19), 3804-3809. doi:10.1002/cssc.201701203

https://hdl.handle.net/10356/141522

https://doi.org/10.1002/cssc.201701203

Effect of FA/Cs Substitution and PbI_2 on the Long Term Stability of Triple Cation Perovskites

Shashwat Shukla[1], Sudhanshu Shukla[1,2], Lew Jia Haur[1], Sai S.H. Dintakurti[2], Guifang Han[1], Anish Priyadarshi[1], Tom Baikie[1], Subodh G. Mhaisalkar[1,2] and Nripan Mathews*[1,2]*

[1]Energy Research Institute @ NTU (ERIAN), Nanyang Technological University, Singapore Research Techno Plaza, 50 Nanyang Drive 637553

[2]School of Materials Science and Engineering, Nanyang Technological University, Singapore, Nanyang Avenue, 639798

E-mail: Subodh@ntu.edu.sg; Nripan@ntu.edu.sg

Abstract: Altering cation and anion ratios in perovskites has been an excellent avenue in tuning the perovskite properties and enhancing the performance. Recently, MA/FA/Cs triple cation mixed halide perovskites have demonstrated efficiencies reaching up to 22 %. Similar to the widely explored MAPbI3, excess PbI2 is added in these perovskite films to enhance the performance. Previous reports demonstrate that the excess PbI2 is beneficial for the performance. However, not much work has been conducted about its impact on stability. Triple cation perovskites (TCP) deploy excess PbI2 up to 8 %. Thus, it is imperative to analyze the role of excess PbI2 in the degradation kinetics. In this paper, we have varied the amount of PbI2 in the triple cation perovskite films and monitored the degradation kinetics by X-ray diffraction (XRD) and optical absorption spectroscopy. We found that the inclusion of excess PbI2 adversely affects the stability of the material. Faster degradation kinetics is observed for higher PbI2 samples. However, excess PbI2 samples showed superior properties such as enhanced grain sizes and better optical absorption. Thus, careful management of the PbI2 quantity is required to obtain better stability and alternative pathways should be explored to achieve better device performance rather than adding excess PbI2.

Introduction

Recently, hybrid organic-inorganic lead halide perovskites (HOIPs) have drawn tremendous attention of the photovoltaic community. Since the inception of photoactive HOIPs with early low efficiency (~3 %) but promising reports in 2009, PV community has grown with an unprecedented rate and revolutionized the development landscape with current record efficiencies reaching over 22 %.[1-7] The vast majority of interest and rapid advancement in this field has put perovskites on par with other developing solar technologies. The prospects of commercialization of these perovskites are extremely bright after encouraging results on large area printed perovskite modules and as a top cell in high efficiency tandem solar cell.[8-13]

In general, these hybrid materials adopt ABX3 perovskite type crystal structure similar to their inorganic counterparts (CaTiO3 etc.) but in this case A being the organic cation at the corners , B metal (Pb) cation at the centre and X anion is the halide (I, Br, Cl) placed at the center of the fcc unit cell forming PbI6 octahedra. The material exhibits an optimal band gap of ~ 1.6 eV and high optical absorption with surprisingly low values of Urbach energy, lower than or comparable to those of highly crystalline materials, obtained for low temperature solution processed thin films.[14, 15] Other advantages include long electron and hole diffusion lengths, high charge carrier mobility, low trap densities and trap-assisted recombination, low non-radiative recombination low exciton binding energy leading to high population of free charge carriers and benign nature of the grain boundaries to the defects.[16-22] All these remarkable properties along with solution processability and easily achievable bandgap tunability through halide substitution has sparked studies on utilizing these materials in other optoelectronics application such as light-emitting diodes (LED), lasers, light emitting field effect transistors and laser cooling.[23-26] Most of these early studies were based on Methylammonium lead halide ($CH_3NH_3PbI_3$) perovskite.

Even though, the efficiencies progressed rapidly, it remained below 20 % and suffered from poor reproducibility. Moreover, these perovskites are continuously marred by the problem of degradation and phase instabilities.[27-30] To address this problem, mixed cation formulation of perovskite was made based on mixture of Methylammonium (MA), Formamidinium (FA) and Cesium (Cs) which resulted in a state-of-the-art perovskite $Cs_{0.05}(MA_{0.15}FA_{0.85})_{0.95}Pb(I_{0.85}Br_{0.15})_3$.[31,32] This triple cation perovskite (TCP) gives the highest efficiency currently (~ 22 %).

The degradation is strongly associated with humidity, temperature, oxygen, light induced changes, chemical reaction at the interface.[33] One noticeable factor in most if not all the high performing cells is the existence of unreacted or excess PbI2 where nominal amount of PbI2 is deliberately added in the perovskite solution to obtain film with excess PbI2.[34-38] While few reports are without excess PbI2.[39, 40] There are several reports on the role of PbI2 on solar cell efficiency.[34, 35, 41-43] Recently, Jacobsson *et al.* have comprehensively studied the impact of PbI2 and argued that excess PbI2 have a profound effect on the charge carrier dynamics and defect passivation manifested by higher efficiencies for PbI2-excess film.[44] Commonly held notions that favour PbI2 inclusion are – passivation at perovskite/TiO2 interface and better energy band alignments facilitating efficient charge transfer, acting as an electron-blocking layer at perovskite/HTL (hole transporting layer) interface helps in grain growth and minimizes the defect states at the grain boundary.[44] Contrarily, there are indications that excess PbI2 might be detrimental from stability point of view.[45] This is particularly important to address, since most of the high efficiency cell formulation deploys 2-8% excess PbI2 in their film, and any intrinsic degradation mechanism involving PbI2 would cause severe damage to the long-term stability of the illuminated cells even after proper encapsulation.

In light of the above, we have evaluated the degradation kinetics of the triple cation perovskite films with varying concentration of excess PbI2 to examine its impact on stability of the film. We chose triple cation film due to two reasons; first, triple cation mixed halide perovskite is the state-of-the-art perovskite used in the record efficiency cell, which is thus far less explored in terms of stability and second, triple cation high efficiency formulation deploys excess PbI2 up to 8 %, which is a significant quantity. By far, most of the degradation studies reported in the literature have been performed on full device, which often lead to the difficulty in deconvolution of degradation caused by environmental factors and due to interfaces in the device itself. Here in this study, we perform all the experiments on perovskite deposited on FTO.

Results and Discussion

Triple cation mixed halide perovskite thin films were prepared by solution processing with varying initial PbI2 concentrations of 0 %, 4 %, 8%, 12 % and 16 %. All five samples were prepared on the transparent conducting fluorine doped tin oxide (FTO) substrate. PbI2 is the common degradation product for the perovskite. Therefore, the rate of its evolution can serve as a marker to track the degradation kinetics. Figure 1 shows a comparison of the X-ray diffraction (XRD) patterns of the as-prepared films and the films obtained after 7 days of exposure to the ambient conditions maintained at a relative humidity of ~ 75 %. In pristine samples, the major reflections could be matched to a tetragonal triple cation perovskite phase reported previously by Dang et al.[46] This confirms that the desired perovskite phase is the predominant phase in all as-prepared films. Except for 0% PbI2 fresh sample, other samples also showed a hexagonal phase corresponding to PbI2, with its most prominent reflection appearing at $2\theta \sim 12.6^{o}$, represented by a star (*) in the Figure 1. It is clear from Figure 1 that the characteristic PbI2 reflection becomes more and more predominant in the diffractograms as excess PbI2 concentration was increased in

the film. No peak shift or additional peak appeared for perovskite suggesting that inclusion of PbI2 does not affect the phase composition of the film and has no solvent effects. However, after 7 days of exposure, an additional and relatively minor reflection was observed at $2\theta \sim 11.6^{o}$. This reflection was found to correspond to a non-perovskite hexagonal δ phase of $FAPbI_3$, as shown by the symbol δ in Figure 1 (a) This is the so-called yellow phase, which is formed from face-sharing PbI_6 octahedra and crystallizes in the space group P63mc.[47] We also attempted to identify any other possible degradation products in light of the previous literature. For single cation standard perovskites, Barnes et al. and Wayland et al. have reported the formation of a hydrated perovskite species MAPbI3.H2O. They have shown that the hydrated species, evolution of PbI2 and partial recovery of MAPbI3 perovskite could be written as following equation [48, 49]

$$4(CH_3NH_3)PbI_3 + 4H_2O \rightleftharpoons 4[CH_3NH_3PbI_3.H_2O] \rightleftharpoons (CH_3NH_3)4PbI_6.2H_2O + 3PbI_2 + 2H_2O$$

And,

$$(CH_3NH_3)_4PbI_6.2H_2O \rightleftharpoons CH_3NH_3PbI_3 + 3CH_3NH_3I + 2H_2O$$

However, the above mechanism cannot be trivially extended to triple cation perovskites (TCP), as no evidence of hydrated species of triple cation perovskite is found in the literature. Hence, we conclude that the hydrated phase analogus to single cation perovskite does not exist in triple-cation perovskite systems.

Optical images corresponding to respective PbI2 concentration are also shown in the Figure 1. The freshly prepared film appears smooth and shiny and changes appearance as PbI2 is increased. Degraded films show random patches at the surface, most likely arising from degradation caused by humidity.

Rietveld refinement XRD analysis was performed using TOPAS 4.1 program to quantify the weight fractions of the perovskite and PbI2 phases and determine how these phases evolve during exposure to high humidity.

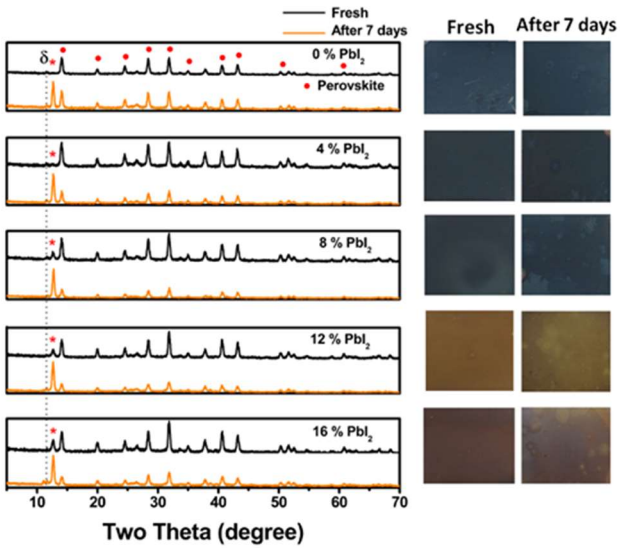

Figure 1. XRD pattern of the triple cation perovskite film on FTO taken for the fresh (0 day) and after 7 days film. * represents PbI2 and δ symbol is for δ -$FAPbI_3$. Right side shows optical image of the fresh and after 7 days sample for the respective films.

Figure 2(a) shows the variation of the weight fraction of the PbI2 and the perovskite phases (PbI2/TCP) with respect to exposure time. It is evident from the figure that this ratio increases with time regardless of the initial PbI2 content, indicating progressive degradation of the perovskite phase and formation of PbI2. However, a comparison of the rate of PbI2 evolution for different samples suggests that compared to other samples, the degradation kinetics is significantly faster for the sample with 8 % excess PbI2. Quantitative XRD analysis reveals another remarkable result – it shows (Figure 2(b)) that similar to degradation kinetics, the total amount of PbI2 formed after degradation also depends on the PbI2 content in the pristine film. First it increases with the increase

in initial PbI2 content, then it reaches a maximum for the 8 % sample, and finally it begins to decrease with any further increase in excess PbI2.

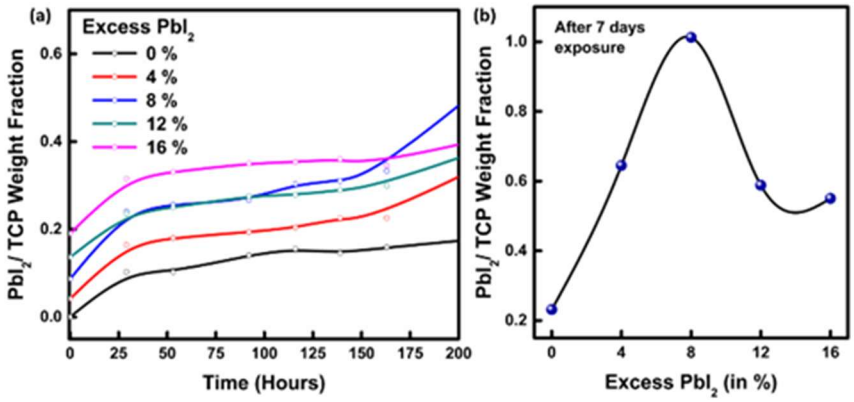

Figure 2. (a) PbI2 XRD peak area as a function of time for the perovskite film with varying PbI2 concentration. (b) Cumulative amount of PbI2 produced after 7 days for films with different amount of initial PbI2 percentage.

Figure 3 shows the change in optical absorption as a function of exposure time for all the perovskite films with different initial concentration of PbI2. 0 % PbI2 sample shows the negligible change upon exposure while 4 % and 8 % film shows decrease in the absorption with band edge becoming less prominent. This could be related to the defect formation and increasing disorder as the film degrades with more PbI2 formation. For 12 % and 16 %, the optical absorption is found to be suppressed. No significant change for the 0 % PbI2 sample substantiates the findings obtained from XRD analysis that the degradation process is slowest for the 0 % PbI2 film.

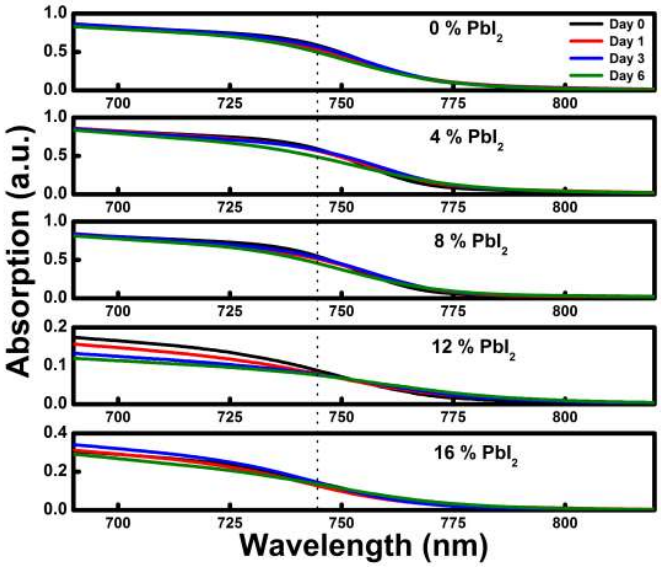

Figure 3. Time evolution of UV-Vis absorption spectra of the triple cation perovskite film on FTO taken for the films with different PbI2 concentration.

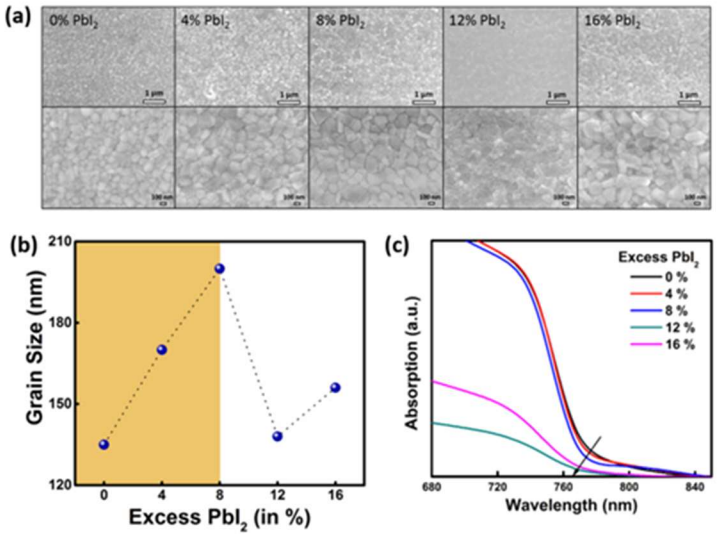

Figure 4. (a) Top view SEM micrographs of the perovskite films having different amount of initial PbI2 concentrations, corresponding high-resolution images are in the bottom of the image. (b) Average grain size estimated from the SEM analysis as function of PbI2 percentage and (c) UV-Vis optical absorption spectra for the pristine fresh films with varying initial PbI2 concentrations.

Top-view SEM images were acquired to investigate the morphology of the films and grain size, (Figure 4 (a)). The films appeared to be smooth and free of pinholes with an increase in grain size as the PbI2 concentration was increased. Average grain size is obtained by statistical analysis of several grains and the value obtained represents the average value of distribution. This is represented in Figure 4(b). It is clear that the grain size increases as PbI2 concentration is increased from 0 % to 8 %, as shown in the yellow region, and then decreases after that for 12 % and 16 % sample, (Figure 4 (b)). The sample with 12 % PbI2 appeared different in the SEM as an exception. However, the overall trend is very clear. In addition, the films tended to be rougher as the PbI2 concentration was increased. Large grain sizes are preferable for devices in order to achieve efficient charge transfer and reduce losses incurred at the grain boundaries due to scattering. The increase in the grain size in our results is consistent with the suggestion that PbI2 assists the grain growth and hence lead to better performance. However, this should be interpreted with caution, as this might not be the only factor responsible for affecting the device performance. Figure 4 (c) shows the optical absorption spectra of the pristine fresh films measured using the integrating sphere. Absorption band edge becomes sharper and shows a blue shift of ~ 5-10 nm as PbI2 increases. However, the 12 % and 16 % samples show a reduced absorption corresponding to perovskite band edge. This is again consistent with the picture that inclusion of PbI2 improves the optoelectronic quality.

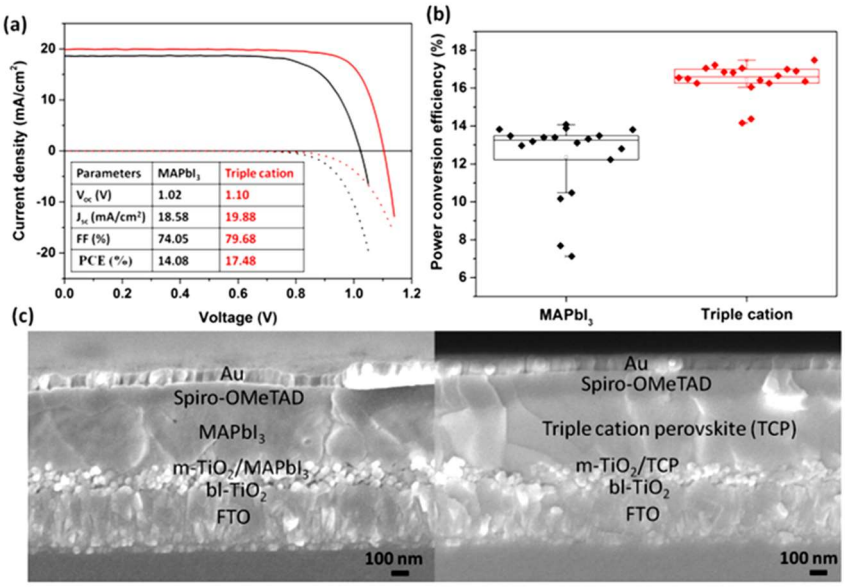

Figure 5. (a) Current-voltage (J-V) characteristics, (b) statistical variation of the PCE of several devices and (c) cross-section SEM micrograph of the CH3NH3PbI3 and Triple cation perovskite solar cell.

To validate the above arguments on the advantageous role of excess PbI2 on device performance, we fabricated solar cells with standard $CH_3NH_3PbI_3$ and triple cation perovskite containing 8 % excess PbI2. It is clear from the current-voltage (J-V) characteristics that TCP cell containing 8 % excess PbI2 performs superior than single cation standard $CH_3NH_3PbI_3$ perovskite, as shown in the dark and light curve in Figure 5 (a). This was further demonstrated by testing several devices as shown in the statistical variation in the photo-conversion efficiency (PCE) of the devices in Figure 5 (b). Device architecture for the both the cells were similar (FTO/compact blocking layer TiO2 (bl-TiO2)/mesoporous TiO2 (m-TiO2)/perovskite/Spiro-OMeTAD/Au) as shown in the cross-section SEM image in Figure 5 (c). It is clear from our results that excess PbI2 in the pristine film is beneficial for obtaining good quality films and consequently better device performance. However, these advantages come at a cost of higher rate of degradation of the film. Therefore, the

focus should be to obtain better properties and efficiency from a stoichiometric film rather than a film containing excess PbI2, which clearly affects the long-term stability of these solar cell devices.

Conclusions

We have investigated the impact of excess PbI2 content on the stability and performance of triple cation perovskite films by monitoring the time evolution of all constituent phases using Rietveld refinement XRD analysis and analyzing the changes in the optical absorption spectra. Our results demonstrate that the amount of PbI2 formed as a result of degradation strongly depends on the initial PbI2 content in the pristine film. It first increases with PbI2 content, then reaches a maxima for 8 % PbI2, and finally starts to decrease at 12 % PbI2, showing a highly non-linear behavior. On the other hand, the optical properties improve and the grain size increases as the initial PbI2 concentration is increased. This implies that inclusion of excess PbI2 offers advantages in terms of better device performance; the downside of this, however, is detrimental for long-term stability of the perovskite itself. Thus, the approach of performance enhancement should focus on stoichiometric films rather than enriching the films with PbI2 and accelerating the degradation. These findings highlight the issues that can influence the long-term device performance and suggests directions towards high efficiency and stable solar cells from triple cation mixed perovskites.

Experimental Section

Perovskite film deposition. All the samples were prepared on FTO glass for the study. FTO substrate was clean thoroughly by three-step sonication in – decon soap cleaning, DI water rinsing and finally dipping in methanol respectively. Thereafter, FTO substrates were subjected to UV

ozone treatment prior to spin coating. Perovskite films were prepared by spin coating the precursors onto a FTO substrate. Triple cation $Cs_{0.05}(MA_{0.15}FA_{0.85})_{0.95}Pb(I_{0.85}Br_{0.15})_3$ perovskite was prepared by mixing the precursors in their respective ratio in a mixed solution of DMF/DMSO (DMF: DMSO=4:1 vv), in 1.35 M concentration. Typically, for 8 % PbI2 film, 0.0504 g of MABr, 0.1816 g of PbBr2, 0.3872 g of FAI and 1.1408 g PbI2 was first dissolved in 2 ml solution of DMF/DMSO solution separately. Cesium containing stock solution was prepared by dissolving CsI in DMSO in 1.5 M concentration. Subsequently, both solutions were mixed to get the desired solution. To obtain the desired stoichiometry, 47.5µl of the stock CsI solution was added to 1.5 ml solution of the mixed cation solution and the resulting solution with a chemical formula of $Cs_{0.05}(MA_{0.15}FA_{0.85})_{0.95}Pb(I_{0.85}Br_{0.15})_3$ is obtained.

Solar cell fabrication. Fluorine doped tin oxide (FTO) glass substrates (Tec15) were cleaned by ultrasonication in a decon soap solution followed by deionized water and ethanol. The cleaned substrates were then treated under UV ozone for 15 min prior to usage. Compact TiO2 (c-TiO2) was spray deposited at 500 °C on a sintering hot plate, using titanium diisopropoxide bis (acetylacetonate) (SigmaAldrich, 75 wt % in isopropanol) mix with isopropanol (SigmaAldrich, anhydrous) and acethylacetone (Sigma-Aldrich). For the Mesoporous TiO2 (mp-TiO2) layer, Dyesol 30NRD was diluted in absolute ethanol in the ratio 1:5.5 (w/w) and then spun onto the substrate at 5500 rpm for 30s. The substrate was then sintered at 500 °C for 15 min. Before device fabrication, 10 mg/mL lithium bis(trifluoromethylsulfonyl) imide solution in acetonitrile (Sigma-Aldrich, anhydrous) was spun on at 3000 rpm for 20s and annealed at 450 °C for 30 min. Triple cation perovskite precursor solution, $Cs_{0.05}(MA_{0.15}FA_{0.85})_{0.95}Pb(I_{0.85}Br_{0.15})_3$ (1.35 M) was prepared by dissolving MABr (Dyesol), PbBr2 (TCI), FAI (Dyesol), and PbI2 (TCI) in a mixture of dimethylformamide (DMF) and dimethyl sulfoxide (DMSO) with a ratio of 4:1 (v/v) at room

temperature for 1 h. CsI in DMSO was added into the perovskite precursor solution to form the composition required. The dissolved perovskite solution was spin-coated on the mpTiO2 layer first at 1000 rpm for 10 s followed immediately by 6000 rpm for 17s. Simultaneously, 0.1 mL of dichlorobenzene was dripped onto the substrate at 13 s. The film was then heated at 100 °C for 1 h in order to obtain black and dense perovskite film. On top of the perovskite layer, a solution of spiro-OMeTAD (70 mg/mL in chlorobenzene), with addition of 4-tert-butylpyridine, lithium bis(trifluoromethylsulfonyl) imide (520 mg/mL in acetonitrile (ACN)), and FK102 (17.2 mg/50 mL of ACN) was spin-coated at 5000 rpm for 30s. All the perovskite and hole transport material (HTM) preparations were done inside a glovebox. Gold back contact (100 nm) was deposited using thermal evaporation.

Film characterization. Thin film X-ray diffraction data was collected by a Bruker D8 Advance diffractometer using Cu Kα radiation. The FE-SEM images were acquired using Jeol JSM-7600F Field Emission Scanning Electron Microscope. UV-Vis optical absorption spectra was aquired using UV-3600 (Shimadzu) spectrophotometer. The J−V measurements were measured using a San-EI Electric, XEC-301S solar simulator under standard simulated AM1.5G illumination, and the light intensity was calibrated using a standard reference silicon cell (Newport).

Acknowledgements

This research was supported by the National Research Foundation, Prime Minister's Office, Singapore under its Competitive Research Programme (CRP Award No. NRF-CRP14-2014-03) and through the Singapore–Berkeley Research Initiative for Sustainable Energy (SinBeRISE) CREATE Program." Authors acknowledge Qian Cheng for his help in Raman measurements.

Keywords: triple cation perovskite • excess PbI2 • degradation • stability • XRD

References

[1] M. A. Green, A. Ho-Baillie, H. J. Snaith, Nat. Photon. 2014, 8, 506.

[2] N. J. Jeon, J. H. Noh, Y. C. Kim, W. S. Yang, S. Ryu, S. I. Seok, Nat. Mater. 2014, 13, 897.

[3] N. J. Jeon, J. H. Noh, W. S. Yang, Y. C. Kim, S. Ryu, J. Seo, S. I. Seok, Nature 2015, 517, 476.

[4] W. Nie, H. Tsai, R. Asadpour, J.-C. Blancon, A. J. Neukirch, G. Gupta, J. J. Crochet, M. Chhowalla, S. Tretiak, M. A. Alam, H.-L. Wang, A. D. Mohite, Science 2015, 347, 522.

[5] J.-P. Correa-Baena, A. Abate, M. Saliba, W. Tress, T. Jesper Jacobsson, M. Gratzel, A. Hagfeldt, Energy Environ. Sci. 2017, 10, 710.

[6] M. A. Green, A. Ho-Baillie, ACS Energy Lett. 2017, 2, 822.

[7] H.-S. Kim, C.-R. Lee, J.-H. Im, K.-B. Lee, T. Moehl, A. Marchioro, S.-J. Moon, R. Humphry-Baker, J.-H. Yum, J. E. Moser, M. Grätzel, N.-G. Park, Sci. Rep. 2012, 2, 591.

[8] A. Priyadarshi, L. J. Haur, P. Murray, D. Fu, S. Kulkarni, G. Xing, T. C. Sum, N. Mathews, S. G. Mhaisalkar, Energy Environ. Sci. 2016, 9, 3687.

[9] M. Yang, Z. Li, M. O. Reese, O. G. Reid, D. H. Kim, S. Siol, T. R. Klein, Y. Yan, J. J. Berry, M. F. A. M. van Hest, K. Zhu, Nat. Energy 2017, 2, 17038.

[10] K. A. Bush, A. F. Palmstrom, Z. J. Yu, M. Boccard, R. Cheacharoen, J. P. Mailoa, D. P. McMeekin, R. L. Z. Hoye, C. D. Bailie, T. Leijtens, I. M. Peters, M. C. Minichetti, N. Rolston, R. Prasanna, S. Sofia, D. Harwood, W. Ma, F. Moghadam, H. J. Snaith, T. Buonassisi, Z. C. Holman, S. F. Bent, M. D. McGehee, Nat. Energy 2017, 2, 17009.

[11] D. Forgács, L. Gil-Escrig, D. Pérez-Del-Rey, C. Momblona, J. Werner, B. Niesen, C. Ballif, M. Sessolo, H. J. Bolink, Adv. Energy Mater. 2017, 7, 1602121.

[12] A. Guchhait, H. A. Dewi, S. W. Leow, H. Wang, G. Han, F. B. Suhaimi, S. Mhaisalkar, L. H. Wong, N. Mathews, ACS Energy Lett. 2017, 2, 807.

[13] G. E. Eperon, T. Leijtens, K. A. Bush, R. Prasanna, T. Green, J. T.-W. Wang, D. P. McMeekin, G. Volonakis, R. L. Milot, R. May, A. Palmstrom, D. J. Slotcavage, R. A. Belisle, J. B. Patel, E. S. Parrott, R. J. Sutton, W. Ma, F. Moghadam, B. Conings, A. Babayigit, H.-G. Boyen, S. Bent, F. Giustino, L. M. Herz, M. B. Johnston, M. D. McGehee, H. J. Snaith, Science 2016.

[14] S. De Wolf, J. Holovsky, S.-J. Moon, P. Löper, B. Niesen, M. Ledinsky, F.-J. Haug, J.-H. Yum, C. Ballif, J. Phys. Chem. Lett. 2014, 5, 1035.

[15] S. D. Stranks, H. J. Snaith, Nat. Nano. 2015, 10, 391.

[16] T. M. Brenner, D. A. Egger, L. Kronik, G. Hodes, D. Cahen, Nat. Energy 2016, 1, 15007.

[17] G. Xing, N. Mathews, S. Sun, S. S. Lim, Y. M. Lam, M. Grätzel, S. Mhaisalkar, T. C. Sum, Science 2013, 342, 344.

[18] D. Shi, V. Adinolfi, R. Comin, M. Yuan, E. Alarousu, A. Buin, Y. Chen, S. Hoogland, A. Rothenberger, K. Katsiev, Y. Losovyj, X. Zhang, P. A. Dowben, O. F. Mohammed, E. H. Sargent, O. M. Bakr, Science 2015, 347, 519.

[19] Q. Dong, Y. Fang, Y. Shao, P. Mulligan, J. Qiu, L. Cao, J. Huang, Science 2015, 347, 967.

[20] S. P. Senanayak, B. Yang, T. H. Thomas, N. Giesbrecht, W. Huang, E. Gann, B. Nair, K. Goedel, S. Guha, X. Moya, C. R. McNeill, P. Docampo, A. Sadhanala, R. H. Friend, H. Sirringhaus, Sci. Adv. 2017, 3.

[21] Y. Chen, H. T. Yi, X. Wu, R. Haroldson, Y. N. Gartstein, Y. I. Rodionov, K. S. Tikhonov, A. Zakhidov, X. Y. Zhu, V. Podzorov, Nat. Commun. 2016, 7, 12253.

[22] D. W. deQuilettes, S. M. Vorpahl, S. D. Stranks, H. Nagaoka, G. E. Eperon, M. E. Ziffer, H. J. Snaith, D. S. Ginger, Science 2015.

[23] S. A. Veldhuis, P. P. Boix, N. Yantara, M. Li, T. C. Sum, N. Mathews, S. G. Mhaisalkar, Adv. Mater. 2016, 28, 6804.

[24] X. Y. Chin, D. Cortecchia, J. Yin, A. Bruno, C. Soci, Nat. Commun. 2015, 6, 7383.

[25] H. Zhu, Y. Fu, F. Meng, X. Wu, Z. Gong, Q. Ding, M. V. Gustafsson, M. T. Trinh, S. Jin, X. Y. Zhu, Nat. Mater. 2015, 14, 636.

[26] S.-T. Ha, C. Shen, J. Zhang, Q. Xiong, Nat. Photon. 2016, 10, 115.

[27] J. A. Christians, P. A. Miranda Herrera, P. V. Kamat, J. Am. Chem. Soc. 2015, 137, 1530.

[28] W. Nie, J.-C. Blancon, A. J. Neukirch, K. Appavoo, H. Tsai, M. Chhowalla, M. A. Alam, M. Y. Sfeir, C. Katan, J. Even, S. Tretiak, J. J. Crochet, G. Gupta, A. D. Mohite, Nat. Commun. 2016, 7, 11574.

[29] T. A. Berhe, W.-N. Su, C.-H. Chen, C.-J. Pan, J.-H. Cheng, H.-M. Chen, M.-C. Tsai, L.-Y. Chen, A. A. Dubale, B.-J. Hwang, Energy Environ. Sci. 2016, 9, 323.

[30] N. H. Tiep, Z. Ku, H. J. Fan, Adv. Energy Mater. 2016, 6, 1501420.

[31] M. Saliba, T. Matsui, J.-Y. Seo, K. Domanski, J.-P. Correa-Baena, M. K. Nazeeruddin, S. M. Zakeeruddin, W. Tress, A. Abate, A. Hagfeldt, M. Gratzel, Energy Environ. Sci. 2016, 9, 1989.

[32] D. P. McMeekin, G. Sadoughi, W. Rehman, G. E. Eperon, M. Saliba, M. T. Hörantner, A. Haghighirad, N. Sakai, L. Korte, B. Rech, M. B. Johnston, L. M. Herz, H. J. Snaith, Science 2016, 351, 151.

[33] S. Wang, Y. Jiang, Emilio J. Juarez-Perez, Luis K. Ono, Y. Qi, Nat. Energy 2016, 2, 16195.

[34] D. H. Cao, C. C. Stoumpos, C. D. Malliakas, M. J. Katz, O. K. Farha, J. T. Hupp, M. G. Kanatzidis, APL Mater. 2014, 2, 091101.

[35] Y. C. Kim, N. J. Jeon, J. H. Noh, W. S. Yang, J. Seo, J. S. Yun, A. Ho-Baillie, S. Huang, M. A. Green, J. Seidel, T. K. Ahn, S. I. Seok, Adv. Energy Mater. 2016, 6, 1502104.

[36] C. Roldan-Carmona, P. Gratia, I. Zimmermann, G. Grancini, P. Gao, M. Graetzel, M. K. Nazeeruddin, Energy & Environmental Science 2015, 8, 3550.

[37] D. Bi, W. Tress, M. I. Dar, P. Gao, J. Luo, C. Renevier, K. Schenk, A. Abate, F. Giordano, J.-P. Correa Baena, J.-D. Decoppet, S. M. Zakeeruddin, M. K. Nazeeruddin, M. Grätzel, A. Hagfeldt, Science Advances 2016, 2.

[38] H.-Y. Wang, M.-Y. Hao, J. Han, M. Yu, Y. Qin, P. Zhang, Z.-X. Guo, X.-C. Ai, J.-P. Zhang, Chemistry – A European Journal 2017, 23, 3986.

[39] U. Thakur, U. Kwon, M. M. Hasan, W. Yin, D. Kim, N. Y. Ha, S. Lee, T. K. Ahn, H. J. Park, 2016, 6, 35994.

[40] J. H. Heo, D. H. Song, H. J. Han, S. Y. Kim, J. H. Kim, D. Kim, H. W. Shin, T. K. Ahn, C. Wolf, T.-W. Lee, S. H. Im, Advanced Materials 2015, 27, 3424.

[41] J. Chang, H. Zhu, J. Xiao, F. H. Isikgor, Z. Lin, Y. Hao, K. Zeng, Q.-H. Xu, J. Ouyang, J. Mater. Chem. A 2016, 4, 7943.

[42] D. Bi, A. M. El-Zohry, A. Hagfeldt, G. Boschloo, ACS Photonics 2015, 2, 589.

[43] H.-S. Ko, J.-W. Lee, N.-G. Park, J. Mater. Chem. A 2015, 3, 8808.

[44] T. J. Jacobsson, J.-P. Correa-Baena, E. Halvani Anaraki, B. Philippe, S. D. Stranks, M. E. F. Bouduban, W. Tress, K. Schenk, J. Teuscher, J.-E. Moser, H. Rensmo, A. Hagfeldt, J. Am. Chem. Soc. 2016, 138, 10331.

[45] F. Liu, Q. Dong, M. K. Wong, A. B. Djurišić, A. Ng, Z. Ren, Q. Shen, C. Surya, W. K. Chan, J. Wang, A. M. C. Ng, C. Liao, H. Li, K. Shih, C. Wei, H. Su, J. Dai, Adv. Energy Mater. 2016, 6, 1502206.

[46] Y. Dang, Y. Liu, Y. Sun, D. Yuan, X. Liu, W. Lu, G. Liu, H. Xia, X. Tao, CrystEngComm 2015, 17, 665.

[47] C. C. Stoumpos, C. D. Malliakas, M. G. Kanatzidis, Inorganic Chemistry 2013, 52, 9019.

[48] G. H. Imler, X. Li, B. Xu, G. E. Dobereiner, H.-L. Dai, Y. Rao, B. B. Wayland, Chem. Commun. 2015, 51, 11290.

[49] A. M. A. Leguy, Y. Hu, M. Campoy-Quiles, M. I. Alonso, O. J. Weber, P. Azarhoosh, M. van Schilfgaarde, M. T. Weller, T. Bein, J. Nelson, P. Docampo, P. R. F. Barnes, Chem. Mater. 2015, 27, 3397.